

# Asteroseismology of the $\beta$ Cephei star $\nu$ Eridani – I. Photometric observations and pulsational frequency analysis

G. Handler,<sup>1\*</sup> R. R. Shobbrook,<sup>2†</sup> M. Jerzykiewicz,<sup>3</sup> K. Krisciunas,<sup>4,5</sup> T. Tshenye,<sup>6</sup> E. Rodríguez,<sup>7</sup> V. Costa,<sup>7</sup> A.-Y. Zhou,<sup>8</sup> R. Medupe,<sup>6,9</sup> W. M. Phorah,<sup>6</sup> R. Garrido,<sup>7</sup> P. J. Amado,<sup>7</sup> M. Paparó,<sup>10</sup> D. Zsuffa,<sup>10</sup> L. Ramokgali,<sup>6</sup> R. Crowe,<sup>11</sup> N. Purves,<sup>11</sup> R. Avila,<sup>11</sup> R. Knight,<sup>11</sup> E. Brassfield,<sup>11</sup> P. M. Kilmartin<sup>12</sup> and P. L. Cottrell<sup>12</sup>

<sup>1</sup>*Institut für Astronomie, Universität Wien, Türkenschanzstrasse 17, A-1180 Wien, Austria*

<sup>2</sup>*Australian National University, Canberra, ACT, Australia*

<sup>3</sup>*Wrocław University Observatory, ul. Kopernika 11, 51-622 Wrocław, Poland*

<sup>4</sup>*Cerro Tololo Inter-American Observatory, National Optical Astronomy Observatory, Casilla 603, La Serena, Chile*

<sup>5</sup>*Las Campanas Observatory, Casilla 601, La Serena, Chile*

<sup>6</sup>*Theoretical Astrophysics Programme, University of the North-West, Private Bag X2046, Mmabatho 2735, South Africa*

<sup>7</sup>*Instituto de Astrofísica de Andalucía, C.S.I.C., Apdo. 3004, 18080 Granada, Spain*

<sup>8</sup>*National Astronomical Observatories, Chinese Academy of Sciences, Beijing 100012, China*

<sup>9</sup>*South African Astronomical Observatory, PO Box 9, Observatory 7935, South Africa*

<sup>10</sup>*Konkoly Observatory, Box 67, H-1525 Budapest XII, Hungary*

<sup>11</sup>*Department of Physics and Astronomy, University of Hawaii - Hilo, 200 West Kawili Street, Hilo, Hawaii, 96720-4091, USA*

<sup>12</sup>*Department of Physics and Astronomy, University of Canterbury, Christchurch, New Zealand*

Accepted 2003 September 12. Received 2003 September 12; in original form 2003 August 4

## ABSTRACT

We undertook a multisite photometric campaign for the  $\beta$  Cephei star  $\nu$  Eridani. More than 600 h of differential photoelectric  $uvyV$  photometry were obtained with 11 telescopes during 148 clear nights.

The frequency analysis of our measurements shows that the variability of  $\nu$  Eri can be decomposed into 23 sinusoidal components, eight of which correspond to independent pulsation frequencies between 5 and 8  $\text{cd}^{-1}$ . Some of these are arranged in multiplets, which suggests rotational  $m$ -mode splitting of non-radial pulsation modes as the cause. If so, the rotation period of the star must be between 30 and 60 d.

One of the signals in the light curves of  $\nu$  Eri has a very low frequency of 0.432  $\text{cd}^{-1}$ . It can be a high-order combination frequency or, more likely, an independent pulsation mode. In the latter case,  $\nu$  Eri would be both a  $\beta$  Cephei star and a slowly pulsating B (SPB) star.

The photometric amplitudes of the individual pulsation modes of  $\nu$  Eri appear to have increased by about 20 per cent over the last 40 years. So have the amplitudes of the dominant combination frequencies of the star. Among the latter, we could only identify sum frequencies with certainty, not difference frequencies, which suggests that neither light-curve distortion in its simplest form nor resonant mode coupling is their single cause.

One of our comparison stars,  $\mu$  Eridani, turned out to be variable with a dominant time-scale of 1.62 d. We believe either that it is an SPB star just leaving its instability strip or that its variations are of rotational origin.

**Key words:** techniques: photometric – stars: early-type – stars: individual:  $\mu$  Eridani – stars: individual:  $\nu$  Eridani – stars: oscillations – stars: variables: other.

\*E-mail: handler@astro.univie.ac.at

†Visiting Fellow.

## 1 INTRODUCTION

Lengthy multisite observations of multiperiodically pulsating stars have become a standard tool in variable star research. The benefits of such efforts are long, uninterrupted time series of the variations of the target stars, which are necessary to resolve complicated pulsational spectra. The more individual variations present in a given pulsator, the more we can learn about its interior by modelling the observed mode spectra. This technique is called asteroseismology.

The most extensive observational efforts for asteroseismology have been performed with dedicated telescope networks. For instance, the Whole Earth Telescope (Nather et al. 1990) has already observed 40 individual targets, more than half of which are pulsating white dwarf stars, the others being pulsating sdB stars, rapidly oscillating Ap stars, cataclysmic variables, etc. The Delta Scuti Network (e.g. Zima et al. 2002) has studied 10 different objects during 23 campaigns and acquired a total of more than 1000 h of measurement for some  $\delta$  Scuti pulsators.

The very first coordinated multisite observations were obtained as early as 1956, on the  $\beta$  Cephei star 12 (DD) Lacertae (de Jager 1963). This effort even included both spectroscopic and multicolour photometric measurements. In more recent times, however,  $\beta$  Cephei stars were (aside from a large campaign for BW Vul; Sterken et al. 1986) rarely the targets of extended observing campaigns. The reason may be the sparse frequency spectra of  $\beta$  Cephei stars compared to pulsating white dwarfs or  $\delta$  Scuti stars. For many years, the record holder was 12 (DD) Lac with five known independent modes of pulsation (Jerzykiewicz 1978), which was recently superseded by the six modes of V836 Cen (Aerts et al. 2003).

However, the apparent paucity of frequencies in the mode spectra of  $\beta$  Cephei stars may be questioned. Experience with  $\delta$  Scuti stars has shown that the more the detection level for periodic light variations is pushed down, the more pulsation modes are detected (e.g. see the sequence of papers by Handler et al. 1996, 1997, 2000). In fact, most of the pulsation modes of these stars have light amplitudes around or below 1 mmag, an amplitude quite easily detected with the large data sets of 2–3 mmag precision differential photometry obtained during these campaigns. As the pulsational driving of the  $\beta$  Cephei stars (Moskalik & Dziembowski 1992) is based on essentially the same mechanism (the  $\kappa$  mechanism) as that of the  $\delta$  Scuti stars, just operating on heavier chemical elements, it can be suspected that many low-amplitude modes are also excited in  $\beta$  Cephei stars but have not yet been detected simply because of a lack of suitable data. Indeed, this idea is supported by recent high-quality observations (Stankov et al. 2002; Cuypers et al. 2002; Handler et al. 2003).

Besides the detection of many pulsation modes, another necessary ingredient for asteroseismology is the correct identification of these modes with their pulsational quantum numbers,  $k$ , the radial overtone of the mode, the spherical degree  $\ell$  and the azimuthal order  $m$ . For pulsating stars whose frequency spectra do not show any obvious regularities caused by rotationally split modes or consecutive radial overtones the use of mode identification methods is required. This may, for instance, be spectroscopic diagnostics from line profile variations or photometric colour amplitude ratios and phase shifts. Unfortunately, such methods may not always yield unambiguous results (see, for example, Balona 2000). However, Handler et al. (2003) recently showed that mode identification from photometric colour amplitudes works well for slowly rotating  $\beta$  Cephei stars and they estimated that a relative accuracy of 3 per cent in the amplitude determinations is sufficient to achieve an unambiguous determination of  $\ell$ .

Consequently,  $\beta$  Cephei stars are indeed suitable for asteroseismic studies. If successful, many interesting astrophysical results can be expected. For instance, angular momentum transport in these stars can be studied. The frequencies of some pulsation modes of  $\beta$  Cephei stars are sensitive to the amount of convective core overshooting (Dziembowski & Pamyatnykh 1991). Deviations from the rotational frequency splitting of non-radial mode multiplets can be due to the interior magnetic field structure of those stars (Dziembowski & Jerzykiewicz 2003). Once the interior structures of several  $\beta$  Cephei stars in various phases of their evolution are determined, main-sequence stellar evolution calculations can be calibrated and more accurately extrapolated to the supernova stage, which can in turn constrain spectral and chemical evolution theories of galaxies.

Hence, it is justified to devote large observational efforts to  $\beta$  Cephei stars that seem suitable for asteroseismology. The selection of a good candidate is one of the most important prerequisites for such a study. For the present work, our choice was  $\nu$  Eri (HD 29248,  $V = 3.92$ ). Its mode spectrum reveals high asteroseismic interest; four pulsation frequencies were known, a singlet and an equally spaced triplet (Kubiak 1980; Cuypers & Goossens 1981). The singlet has been suggested to be a radial mode, and the triplet is consistent with a dipole (Aerts, Waelkens & de Pauw 1994; Heynderickx, Waelkens & Smeyers 1994).

If this triplet contained at least two rotationally split  $m$ -components of a mode,  $\nu$  Eri would also be a slow rotator, a hypothesis supported by its measured  $\nu \sin i$  (the most recent determination being  $20 \text{ km s}^{-1}$ ; Abt, Levato & Grosso 2002). This is important because the adverse effects of rotational mode coupling (see Pamyatnykh 2003 or Daszyńska-Daszkiewicz et al. 2002) in a subsequent theoretical analysis would be diminished. Finally,  $\nu$  Eri is a bright equatorial star, so it can be observed from both hemispheres with photometric and high-resolution spectroscopic instruments.

We therefore organized a multisite campaign for  $\nu$  Eri, applying both observing methods mentioned above (Handler & Aerts 2002). In the following, we report on the results from the photometric measurements. The analysis of the spectroscopy, pulsational mode identification and seismic modelling of the identified oscillations will be the subject of future papers.

## 2 OBSERVATIONS AND REDUCTIONS

Our photometric observations were carried out with 11 different telescopes and photometers at 10 observatories on five different continents; these are summarized in Table 1. In most cases, single-channel differential photometry was acquired through the Strömrgren *uvv* filters. However, at Sierra Nevada Observatory (OSN) a simultaneous *uvby* photometer was used, so we included the *b* filter as well, and at the four observatories where no Strömrgren filters were available we used Johnson *V*. Some measurements through the  $H_\beta$  filters were also obtained at OSN. The total time base line spanned by our measurements is 157.9 d.

We chose two comparison stars for  $\nu$  Eri:  $\mu$  Eri (HD 30211, B5IV,  $V = 4.00$ ) and  $\xi$  Eri (HD 27861, A2V,  $V = 5.17$ ). Another check star, HD 29227 (B7 III,  $V = 6.34$ ) was also monitored at OSN. We note that  $\mu$  Eri was the single comparison star in all published extensive photometric studies of  $\nu$  Eri (van Hoof 1961; Kubiak & Seggewiss 1991) and that its *Hipparcos* photometric data (ESA 1997) imply some slow variability (Koen & Eyer 2002). The star is also a spectroscopic binary ( $P_{\text{orb}} = 7.35890 \text{ d}$ ,  $e = 0.26$ ; Hill 1969). In the hope that we could also understand the variability of  $\mu$  Eri with our multisite observations, and hoping to use that knowledge

**Table 1.** Log of the photometric measurements of  $\nu$  Eri. Observatories are ordered according to geographical longitude. Sites that acquired  $V$  measurements only are marked with asterisks.

Observatory	Longitude	Latitude	Telescope	Amount of data Nights	h	Observer(s)
Sierra Nevada Observatory	$-3^{\circ} 23'$	$+37^{\circ} 04'$	0.9-m	18	53.59	ER, VC, RG, PJA
Cerro Tololo Interamerican Observatory	$-70^{\circ} 49'$	$-30^{\circ} 09'$	0.6-m	8	43.19	KK
Fairborn Observatory	$-110^{\circ} 42'$	$+31^{\circ} 23'$	0.75-m APT	24	114.54	–
Lowell Observatory	$-111^{\circ} 40'$	$+35^{\circ} 12'$	0.5-m	10	46.01	MJ
Mauna Kea Observatory*	$-155^{\circ} 28'$	$+19^{\circ} 50'$	0.6-m	4	7.78	RC, NP, RA, RK, EB
Mount John University Observatory*	$+170^{\circ} 28'$	$-43^{\circ} 59'$	0.6-m	1	3.83	PMK
Siding Spring Observatory	$+149^{\circ} 04'$	$-31^{\circ} 16'$	0.6-m	31	117.70	RRS
Xing-Long Observatory*	$+117^{\circ} 35'$	$+40^{\circ} 24'$	0.85-m	3	15.72	AYZ
South African Astronomical Observatory	$+20^{\circ} 49'$	$-32^{\circ} 22'$	0.5-m	37	151.82	GH, TT, RM, WP, LR
South African Astronomical Observatory	$+20^{\circ} 49'$	$-32^{\circ} 22'$	0.75-m	7	39.31	GH
Piszkestető Observatory*	$+19^{\circ} 54'$	$+47^{\circ} 55'$	0.5-m	5	11.86	MP, DZ
Total				148	605.35	

in re-analyses of the published data of  $\nu$  Eri, we retained  $\mu$  Eri as a comparison star. During data reduction, we took care that the variations of  $\mu$  Eri would not influence the results on our primary target.

Data reduction was therefore started by correcting for coincidence losses, sky background and extinction. Nightly extinction coefficients were determined with the Bouguer method from the  $\xi$  Eri measurements only; second-order colour extinction coefficients were also determined. We then calculated differential magnitudes between the comparison stars (in the sense  $\mu$  Eri– $\xi$  Eri). Heliocentrically corrected versions of these time series were set aside for later analysis of the variability of  $\mu$  Eri, to which we will return later.

The nightly ( $\mu$  Eri– $\xi$  Eri) differential magnitudes were fitted with low-order polynomials ( $n < 4$ ). The residuals of the non-differential  $\mu$  Eri magnitudes with respect to that fit were combined with the  $\xi$  Eri data and were assumed to reflect the effects of transparency and detector sensitivity changes only. Consequently, these combined time series were binned into intervals that would allow good compensation for the above-mentioned non-intrinsic variations in the target star time series and were subtracted from the measurements of  $\nu$  Eri. The binning minimizes the introduction of noise in the differential light curve of the target.

The timings for this differential light curve were heliocentrically corrected as the next step. Finally, the photometric zero-points of the different instruments, which may be different because of the different colours of  $\nu$  Eri and  $\xi$  Eri, were examined at times of overlap with a different site and adjusted if necessary. Measurements in the Strömgren  $y$  and Johnson  $V$  filters were treated as equivalent and analysed together due to the same effective wavelength of these filters. The resulting final combined time series was subjected to frequency analysis; we show some of our light curves of  $\nu$  Eri in Fig. 1. In the end, we had more than 3000 measurements in each filter with accuracies of 3.7 ( $u$  filter), 3.0 ( $v$  filter) and 3.0 mmag ( $y/V$  filters) per data point available.

### 3 FREQUENCY ANALYSIS

#### 3.1 The programme star

Our frequency analyses were mainly performed with the program PERIOD 98 (Sperl 1998). This package applies single-frequency power spectrum analysis and simultaneous multifrequency sine-wave fitting. It also includes advanced options, such as the calcu-

lation of optimal light-curve fits for multiperiodic signals including harmonic, combination, and equally spaced frequencies. As will be demonstrated later, our analysis requires some of these features.

We started by computing the Fourier spectral window of the final light curves in each of the filters. It was calculated as the Fourier transform of a single noise-free sinusoid with a frequency of  $5.7633 \text{ cd}^{-1}$  (the strongest pulsational signal of  $\nu$  Eri) and an amplitude of 36 mmag sampled in the same way as were our measurements. The upper panel of Fig. 2 contains the result for the combined  $y$  and  $V$  data. Any alias structures that would potentially mislead us into incorrect frequency determinations are quite low in amplitude due to our multisite coverage.

We proceeded by computing the amplitude spectra of the data itself (second panel of Fig. 2). The signal designated  $f_1$  dominates, but some additional structures not compatible with the spectral window side lobes are also present. Consequently, we pre-whitened this signal by subtracting a synthetic sinusoidal light curve with a frequency, amplitude and phase that yielded the smallest possible residual variance, and computed the amplitude spectrum of the residual light curve (third panel of Fig. 2).

This resulted in the detection of a second signal ( $f_2$ ) and of another variation at the sum frequency of the two previously detected. We then pre-whitened a three-frequency fit from the data using the same optimization method as before and fixed the combination term to the exact sum of the two independent frequencies. We continued this procedure (further panels of Fig. 2) until no significant peaks were left in the residual amplitude spectrum.

We consider an independent peak statistically significant if it exceeds an amplitude signal-to-noise ratio ( $S/N$ ) of 4 in the periodogram; combination signals must satisfy  $S/N > 3.5$  to be regarded as significant (see Breger et al. 1999, for a more in-depth discussion of this criterion). The noise level was calculated as the average amplitude in a  $5\text{-cd}^{-1}$  interval centred on the frequency of interest.

We repeated the pre-whitening procedure with the  $u$  and  $v$  data independently and obtained the same frequencies within the observational errors. We then determined final values for the detected frequencies by averaging the values from the individual filters, weighted by their  $S/N$ . The pulsational amplitudes were then re-computed with those frequencies; the result is listed in Table 2.

The residuals from this solution were searched for additional candidate signals that may be intrinsic. We have first investigated the residuals in the individual filters, then analysed the averaged residuals in the three filters (whereby the  $u$  data were divided by 1.5 to scale them to amplitudes and rms scatter similar to that in the

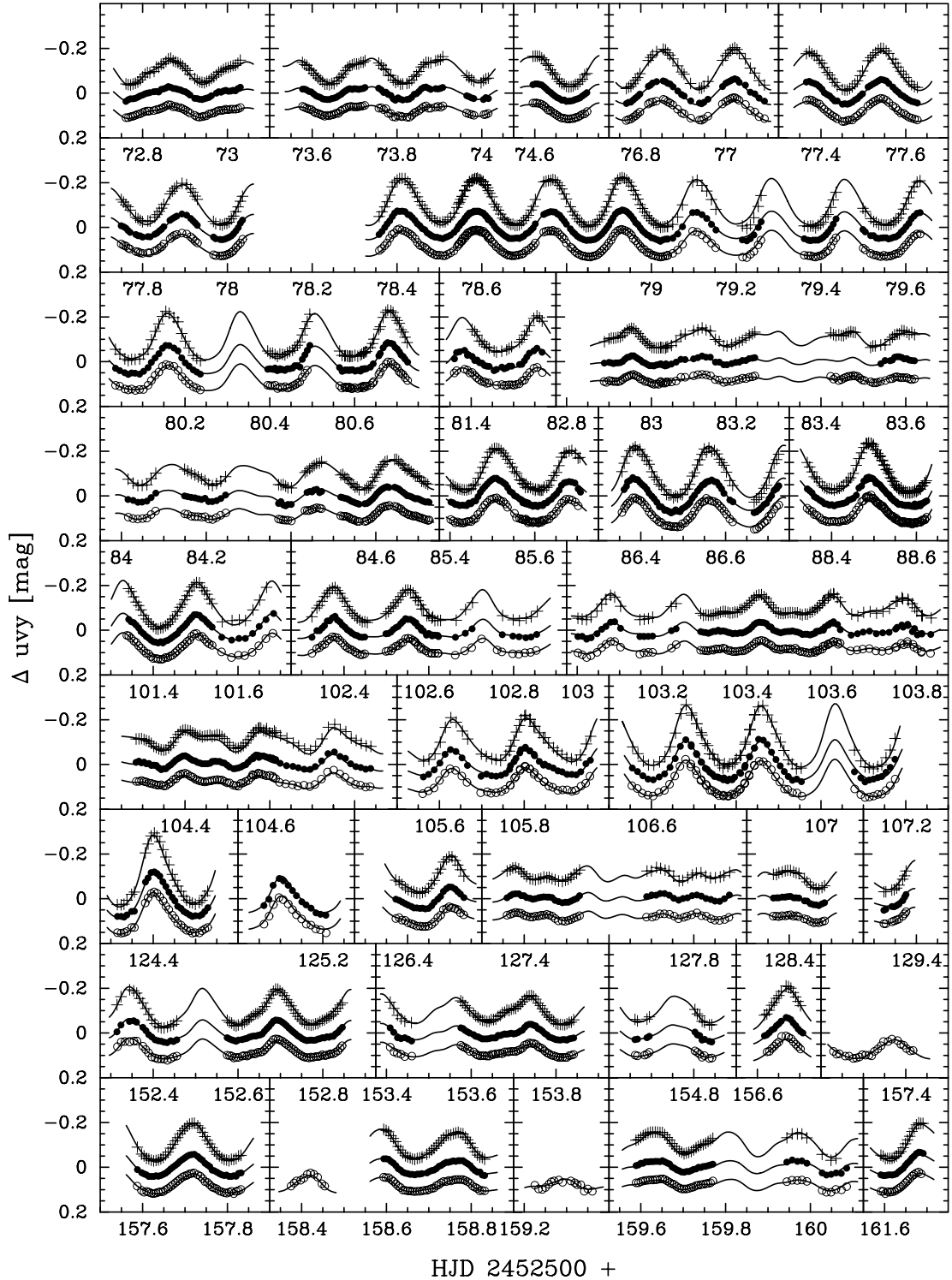


**Figure 1.** Some light curves of  $\nu$  Eri. Plus signs are data in the Strömgren  $u$  filter, filled circles are our  $v$  measurements and open circles represent Strömgren  $y$  and Johnson  $V$  data. The full line is a fit composed of all the periodicities detected in the light curves (Table 2). The amount of data shown here is about half the total.

other two filters), and finally applied statistical weights according to the recommendation by Handler (2003). Some interesting features were found and are listed in Table 3.

In this table, the signal at  $0.254 \text{ cd}^{-1}$  is formally significant in the  $v$  filter data, and noticeable peaks are present at the same frequency

in both the  $u$  and  $y$  filter data. However, we find the evidence from all the data sets taken together not sufficiently convincing to claim reality for this peak. Similar comments apply to the other signals listed in Table 3. We would, however, like to point out that the variations near  $6\text{--}8 \text{ cd}^{-1}$  may all be components of multiplets that

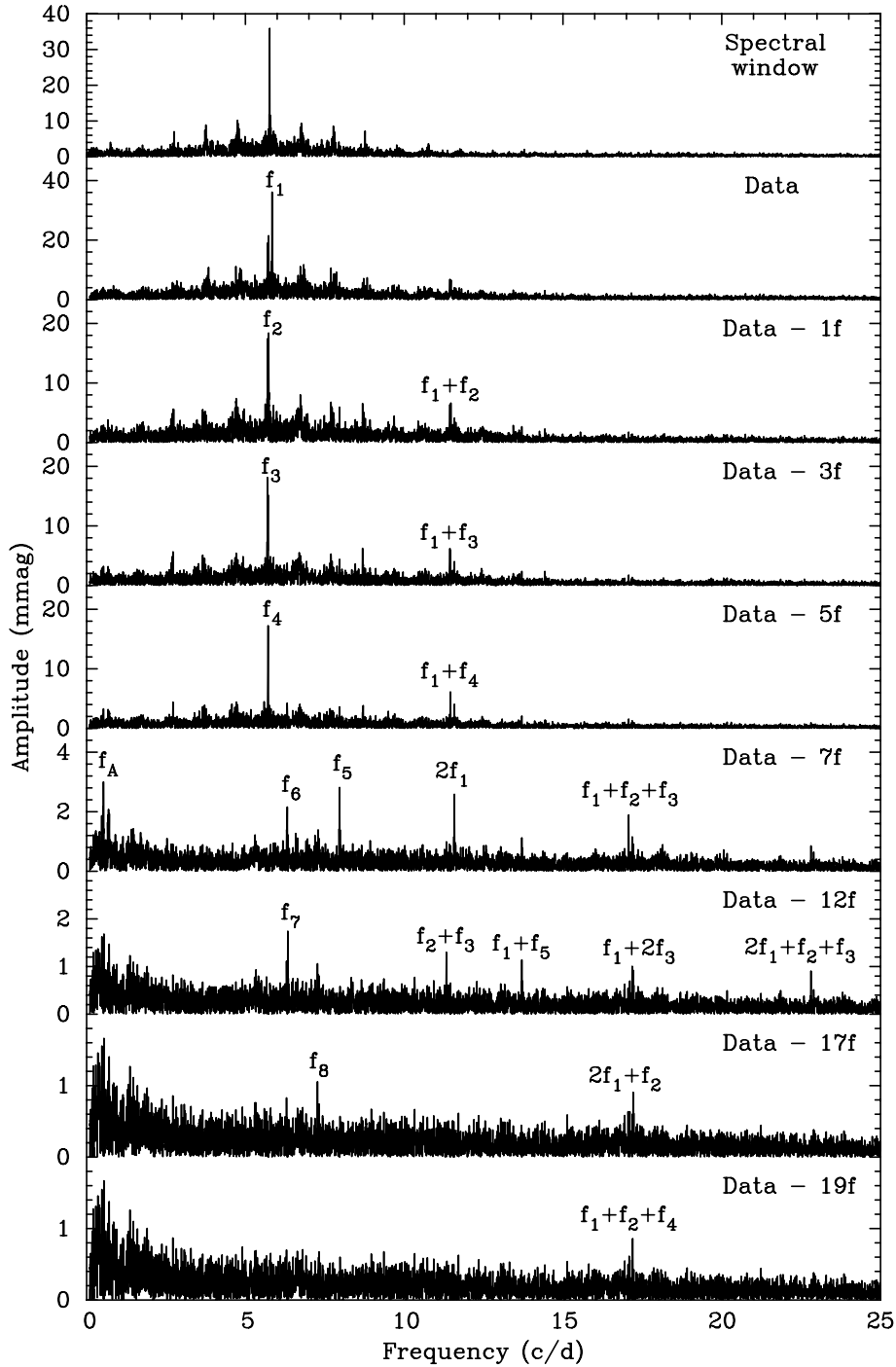


**Figure 2.** Amplitude spectra of  $\nu$  Eri. The uppermost panel shows the spectral window of the data, followed by the periodogram of the data. Successive pre-whitening steps are shown in the following panels; note their different ordinate scales. See text for details.

include detected modes. The signals at frequencies higher than  $17 \text{ cd}^{-1}$  all coincide with combinations of detected modes.

### 3.2 The comparison stars

We still have to analyse the light curves of  $\mu$  Eri– $\xi$  Eri. To this end, we have computed the amplitude spectrum of these data and show it in the upper panel of Fig. 3. One peak stands out; pre-whitening it leaves strong evidence for further variability of this star (Fig. 3, second panel), but no more periodicities can be detected.

The single periodicity that may be present in the light curves of  $\mu$  Eri has a frequency of  $0.61638 \pm 0.0005 \text{ cd}^{-1}$  and  $uvy$  amplitudes of 10.2, 6.4 and 5.0 mmag, respectively. It is statistically significant with S/N ratios between 6.3 and 4.4 in the different filters, but it is not clear if its frequency and amplitude were constant throughout the observing window. The residual amplitude spectrum after pre-whitening this signal still shows a very strong  $1/f$  component and indicates that the variability of  $\mu$  Eri is complicated. However, further analyses of the differential  $\mu$  Eri– $\xi$  Eri light curves, such as searching for variations with non-sinusoidal pulse shapes using

**Table 2.** Multifrequency solution for our time-resolved photometry of  $\nu$  Eri. Formal error estimates (following Montgomery & O’Donoghue 1999) for the independent frequencies range from  $\pm 0.00001$   $\text{cd}^{-1}$  for  $f_1$  to  $\pm 0.00035$   $\text{cd}^{-1}$  for  $f_8$ . Formal errors on the amplitudes are  $\pm 0.2$  mmag in  $u$  and  $\pm 0.1$  mmag in  $v$  and  $y$ . The S/N ratio quoted is for the  $y$  filter data.

ID	Freq. ( $\text{cd}^{-1}$ )	$u$ ampl. (mmag)	$v$ ampl. (mmag)	$y$ ampl. (mmag)	S/N
$f_1$	5.76327	73.5	41.0	36.9	137.0
$f_3$	5.62006	34.6	23.9	22.7	83.6
$f_4$	5.63716	32.2	22.4	21.0	77.7
$f_2$	5.65393	37.9	26.4	25.1	92.6
$f_6$	6.24408	3.9	2.5	2.6	9.8
$f_7$	6.26205	2.9	1.9	1.8	6.8
$f_8$	7.19994	1.3	0.9	1.1	4.3
$f_5$	7.89780	4.3	3.1	3.0	11.7
$f_A$	0.43218	5.5	3.2	3.2	7.1
$f_2 + f_3$	11.27399	2.8	1.7	1.4	6.4
$f_1 + f_3$	11.38333	11.1	7.9	7.5	34.9
$f_1 + f_4$	11.40043	10.9	7.7	7.1	33.2
$f_1 + f_2$	11.41720	12.6	9.0	8.4	39.3
$2f_1$	11.52654	4.5	3.1	2.9	13.8
$f_1 + f_5$	13.66107	1.6	1.2	1.1	6.4
$f_1 + f_3 + f_4$	17.02049	1.0	0.7	0.7	4.7
$f_1 + f_2 + f_3$	17.03726	4.4	3.1	2.6	16.9
$f_1 + f_2 + f_4$	17.05435	1.0	0.8	0.9	6.1
$f_1 + 2f_2$	17.07113	0.8	0.7	0.5	3.5
$2f_1 + f_3$	17.14660	1.8	1.4	1.2	8.0
$2f_1 + f_4$	17.16370	1.7	1.2	1.0	6.6
$2f_1 + f_2$	17.18047	1.9	1.4	1.3	8.2
$2f_1 + f_2 + f_3$	22.80053	1.5	1.0	0.9	6.9

**Table 3.** Possible further signals. The data set in which they attained highest S/N are indicated.

ID	Frequency ( $\text{cd}^{-1}$ )	S/N
	0.2543	4.0 ( $v$ )
	6.221	3.6 ( $uvy$ , weighted)
	7.252	3.4 ( $uvy$ , weighted)
	7.914	3.1 ( $u$ )
$f_1 + 2f_3$	17.0034	3.2 ( $u$ )
$f_1 + 2f_2 + f_3$	22.6912	3.5 ( $u$ )
$3f_1 + f_2 + f_3$	28.5638	3.1 ( $u$ )

the residualgram method (Martinez & Koen 1994) or by folding the data with the orbital period, all remained inconclusive.

On the other hand, we noticed that the amplitude spectrum of the de-trended comparison star magnitude differences (with a low-order polynomial fitted to each night of data to remove the slow variability of  $\mu$  Eri) has the highest peak at  $10.873$   $\text{cd}^{-1}$  in all the filters. It is even significant with a S/N = 5.2 in the  $v$  filter data, where it reaches an amplitude of 0.6 mmag.

To examine whether this peak is real and, if so, from what star it originates, we computed the differential ( $\nu$  Eri– $\mu$  Eri) and ( $\nu$  Eri– $\xi$  Eri) light curves. We then pre-whitened the frequency solution from Table 2 from these data and computed the residual amplitude spectra. We also examined the ( $\xi$  Eri–HD 29227) data from OSN for this purpose. Unfortunately, these tests were not fully conclusive because the noise level in these amplitude spectra is higher than in those of the de-trended differential comparison star magnitudes

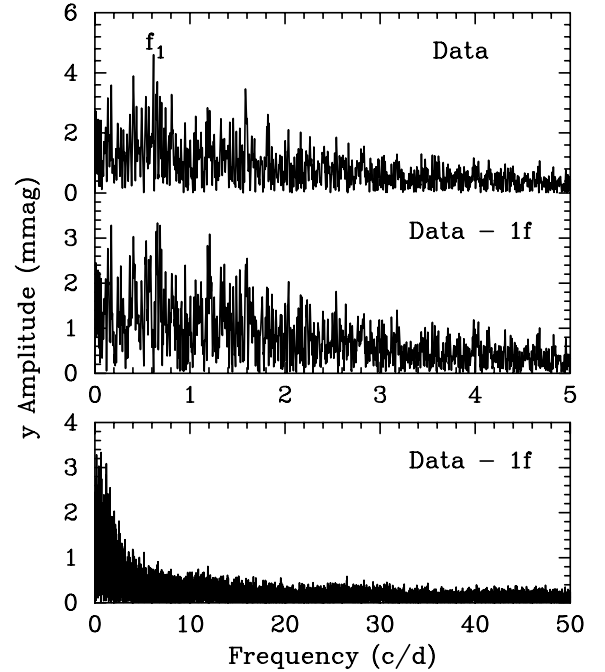


**Figure 3.** Upper panel: amplitude spectrum of ( $\mu$  Eri– $\xi$  Eri) in the  $y$  filter. Second panel: residual amplitude spectrum after pre-whitening  $f_1$ . Lower panel: residual amplitude spectrum of ( $\mu$  Eri– $\xi$  Eri) out to the Nyquist frequency; no further variations are detected.

only. All we can say is that, if real, the  $10.873$ - $\text{cd}^{-1}$  variation is more likely to originate from  $\xi$  Eri. In any case, our assumption that  $\xi$  Eri is photometrically constant does not affect our analysis of  $\nu$  Eri.

### 3.3 Re-analysis of literature data

We have re-analysed the photometric measurements by van Hoof (1961) and Kubiak & Seggewiss (1991). The first data set was retrieved from the IAU archives (as deposited by Cuypers & Goossens 1981) and consists of two seasons of ultraviolet  $U$  and one season of yellow  $Y$  measurements (the  $Y$  bandpass is identical to Johnson  $V$ ; see Lyngå 1959). The frequency analysis was performed on the  $U$  data as they are considerably more numerous, whereas we determined only the amplitudes in the  $Y$  data with frequencies fixed to the values derived from the  $U$  measurements.

We homogenized these data by averaging them into 7-min bins and by removing poor data, sometimes whole nights. The frequency analysis of the resulting  $U$  data set revealed the presence of frequencies  $f_1$  to  $f_4$  as well as the sum frequencies of  $f_1$  with the  $f_2, f_3, f_4$  triplet. The amplitude spectrum after pre-whitening the corresponding multifrequency fit shows a strong increase of noise that precludes the detection of further signals. We note that neither the low  $0.432$ - $\text{cd}^{-1}$  variation of  $\nu$  Eri nor the suspected  $0.616$ - $\text{cd}^{-1}$  periodicity of  $\mu$  Eri could be detected.

To enable a search for further signals known from our analysis in those data, we determined the zero-points of the residual light curves of the individual nights and subtracted them from the data. Fourier analysis of this modified data set allowed the detection of four more signals established in our measurements. Their frequencies and amplitudes recovered in van Hoof’s  $U$  data are listed in Table 4 together with the corresponding  $Y$  amplitudes.

The photometric measurements by Kubiak & Seggewiss (1991) consist of two runs of 17.1-d and 5.1-d time base, respectively,

**Table 4.** Multifrequency solution for the  $U$  and  $Y$  data of van Hoof (1961). The identifications of the signals are the same as in Table 2. Formal error estimates (Montgomery & O’Donoghue 1999) for the independent frequencies range from  $\pm 0.00001 \text{ cd}^{-1}$  for  $f_1$  to  $\pm 0.00017 \text{ cd}^{-1}$  for  $f_6$ . Formal errors on the  $U$  amplitudes are  $\pm 0.3 \text{ mmag}$ . However, the real errors are believed to be higher because of the zero-point adjustments we made. The formal uncertainty on the  $Y$  amplitudes is  $\pm 0.8 \text{ mmag}$ .

ID	Freq. ( $\text{cd}^{-1}$ )	$U$ ampl. (mmag)	$Y$ ampl. (mmag)	S/N
$f_1$	5.76345	52.8	28.9	78.2
$f_3$	5.62018	25.5	20.1	37.7
$f_4$	5.63738	26.5	19.5	39.2
$f_2$	5.65385	27.9	20.8	41.3
$f_6$	6.24417	2.7	2.1	4.0
$f_7$	6.26227	3.7	4.0	5.6
$f_5$	7.89830	2.1	2.0	3.1
$f_1 + f_3$	11.38363	8.1	6.2	13.0
$f_1 + f_4$	11.40083	8.1	5.5	13.0
$f_1 + f_2$	11.41730	9.2	7.0	14.7
$2f_1$	11.52690	2.8	3.8	4.4

separated by 4 yr. The  $f_2, f_3, f_4$  triplet can, therefore, not be resolved in these data, but  $f_1$  can be separated from it and its  $uvby$  amplitudes can be estimated. We obtain amplitudes of  $55 \pm 3 \text{ mmag}$  in  $u$ ,  $30 \pm 2 \text{ mmag}$  in  $v$ ,  $28 \pm 2 \text{ mmag}$  in  $b$  and  $27 \pm 2 \text{ mmag}$  in  $y$  for signal  $f_1$ . The  $0.616\text{-cd}^{-1}$  variation of  $\mu$  Eri may be present in these data.

## 4 DISCUSSION

### 4.1 The $\beta$ Cephei type pulsation frequencies

We have detected eight independent signals in the light curves of  $\nu$  Eri that are in the typical frequency domain for  $\beta$  Cephei star pulsation, i.e. they are pressure (p) and gravity (g) modes of low radial order. We show the schematic amplitude spectrum composed of these modes and of further suspected signals in Fig. 4.

This figure shows intriguing structures. Besides the known triplet of frequencies near  $5.64 \text{ cd}^{-1}$ , there is another doublet near  $6.24 \text{ cd}^{-1}$  with a suspected further component, and the two other signals near  $7.2$  and  $7.9 \text{ cd}^{-1}$  may also be parts of mode multiplets. We believe that these are signs of rotational splitting of non-radial pulsation modes. If so, the rotation period of  $\nu$  Eri must be between 30 and 60 d, depending on the types of mode we see (p and/or g modes).

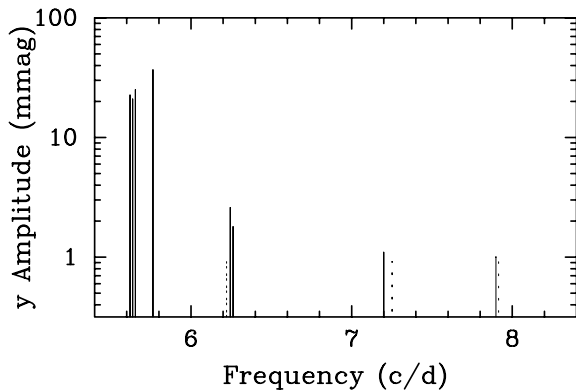


**Figure 4.** Schematic amplitude spectrum of  $\nu$  Eri. The solid lines represent detected modes, whereas the dashed lines indicate the positions of possible further signals.

The low-frequency triplet is asymmetric. Dziembowski & Jerzykiewicz (2003) calculated the asymmetry as  $A_{\text{obs}} = f_2 + f_3 - 2f_4 = -7.1 \pm 0.3 \times 10^{-4} \text{ cd}^{-1}$  (using the naming convention from Table 2) from archival data, whereas our measurements indicate  $A_{\text{obs}} = -3.3 \pm 0.4 \times 10^{-4} \text{ cd}^{-1}$ . Comparing Tables 2 and 4, it appears that our value for the triplet centroid frequency  $f_4$  is less accurate than the formal errors would suggest – which is plausible given that our observational time base is only about 2.6 times the inverse triplet splitting.

A comparison of Tables 2 and 4 allows another interesting conclusion; the pulsational amplitudes of all modes of  $\nu$  Eri seem to have increased between the measurements of van Hoof and those of our studies. Allowing for the different wavelength passband of the archival  $U$  measurements that also included a silvered mirror (Lyngå 1959) and our Strömgren  $u$  data, an increase in the pulsational amplitudes of about 20 per cent can be estimated. It is possible that most of this increase has occurred in the last 15–20 yr as the  $u$  amplitude of  $f_1$  in the data by Kubiak & Seggewiss (1991) is also considerably smaller than in our data.

### 4.2 The combination signals

The light curves of  $\nu$  Eri are not perfectly sinusoidal (cf. Fig. 1); therefore, combination signals result from our method of frequency determination. It is not well known what the physical cause of combination frequencies is. Some of the most prominent hypotheses include simple light-curve distortions due to the pulsations propagating in a non-linearly responding medium or independent pulsation modes excited by resonances.

In case of the light-curve distortion hypothesis, the amplitudes and phases of the combination frequencies can be predicted. They also contain some information about the medium that distorts the light curves (see Wu 2001 and references therein). In the simplest case, the amplitudes of the combination signals scale directly with the product of the amplitudes of the parent modes (see, for example, Garrido & Rodríguez 1996).

As we do not have a pulsational mode identification available at this point, we cannot examine the two above-mentioned hypotheses quantitatively, but some statements can still be made. For instance, simple light-curve distortion should produce combination sum and difference frequencies of about the same amplitude. However, difference frequencies are completely absent in our multifrequency solution (Table 2) although the strongest of these signals should be easily detectable in our data.

The amplitude variations we reported before can also be examined. We note that the amplitude of the sum frequencies of  $f_1$  with the  $f_2, f_3, f_4$  triplet increased by about 20 per cent, which is the same as the increase of the individual amplitudes of the parent modes, but less than expected for the simple light-curve distortion hypothesis.

The absence of the difference frequencies also poses a problem for the resonant mode coupling hypothesis. As the stellar eigenmode spectrum is much denser at low frequencies than at high frequencies due to the presence of many gravity modes, we would expect to see many more difference frequencies in the case of mode coupling, which is not the case.

### 4.3 The low-frequency variation

We found a signal of  $0.43218 \text{ cd}^{-1}$  in the light curves of  $\nu$  Eri and evidence for other periodic low-frequency signals. Such variability is an order of magnitude slower than  $\beta$  Cephei type pulsation. These variations are not due to the slowly variable comparison star  $\mu$  Eri;

they occur at frequencies different from the dominant variation of the latter star and we have taken care that its variability does not affect our analysis of  $\nu$  Eri in our reduction procedures. They are, therefore, present in our light curves of  $\nu$  Eri.

Although this slow variability has been detected in the measurements in all three Strömgen filters used, we have taken special care in determining whether these variations are intrinsic to the star. Consequently, we computed amplitude spectra of the four largest homogeneous subsets of data (i.e. those that used the same filters and detectors throughout the whole campaign and that spanned a time base longer than 70 d) in all three filters. We have found a peak at  $0.432 \text{ cd}^{-1}$  present in all these amplitude spectra, and we are therefore sure it is not an artefact of the observing or reduction procedures; it is due to intrinsic variations of  $\nu$  Eri.

Unfortunately, there is some doubt as to whether this is an independent frequency or not. A possible high-order combination frequency ( $3f_1 - 3f_3$ ) would be located only  $0.0026 \text{ cd}^{-1}$  away from  $f_A$ , which is much larger than the formal error estimate of  $\pm 0.0001 \text{ cd}^{-1}$  for the frequency uncertainty of  $f_A$ , but smaller than the  $0.0063\text{-cd}^{-1}$  frequency resolution of our data. It would be surprising if such a high-order difference frequency were present in our data when there is no evidence for lower-order ones. We thus suspect that  $f_A$  is an independent frequency, but only new measurements increasing the time base of our data set will allow us to answer this question unambiguously.

If  $f_A$  were an independent periodicity, what would be the physical reason for such a variability? As argued above, the rotation period of  $\nu$  Eri must be between 30 and 60 d; the observed 2.3-d period can therefore not be connected to rotation.  $\nu$  Eri is also not known to be a binary; extensive radial velocity studies are available and no variability except that due to the short-period pulsations has ever been reported. In addition, the wavelength dependence of the amplitude of the  $0.432\text{-cd}^{-1}$  signal excludes a pure geometric origin of this variability.

Hence, the slow variations are probably due to high-order g-mode pulsations of the star, which is also consistent with the colour amplitudes. We note that Jerzykiewicz (1993) also detected a low-frequency variation in his light curves of the  $\beta$  Cephei star 16 (EN) Lac, which he interpreted to be either due to a pair of spots – or due to g-mode pulsation.

#### 4.4 The variability of $\mu$ Eri

In Section 3.1 we reported that one of our comparison stars,  $\mu$  Eri, shows rather complex light variations with a time-scale of about 1.6 d. To examine their origin, we first determined its position in the Hertzsprung–Russell (HR) diagram. As a start, we retrieved the standard Strömgen and Geneva colours of  $\mu$  Eri from the Lausanne–Geneva data base (<http://obswww.unige.ch/gcpd/gcpd.html>).

The star’s Geneva colours then imply  $T_{\text{eff}} = 15\,670 \pm 100 \text{ K}$  according to the calibrations by Künzli et al. (1997). The star’s *Hipparcos* parallax (ESA 1997), combined with a reddening correction of  $A_V = 0.06$  determined from its Strömgen colours and the calibration of Crawford (1978), the bolometric corrections by Flower (1996) and Drilling & Landolt (2000) result in  $M_{\text{bol}} = -3.6 \pm 0.4$ . We can thus place  $\mu$  Eri in the theoretical HR diagram (Fig. 5).

Interestingly,  $\mu$  Eri seems to be an object just at or shortly after the end of its main-sequence life. It is located within the instability strip of the SPB stars, and the time-scale (cf. De Cat & Aerts 2002; Pamyatnykh 2002) and complexity of its variability as well as the colour dependence of its amplitudes on wavelength are consistent with it being an SPB star.  $\mu$  Eri may have many pulsation modes

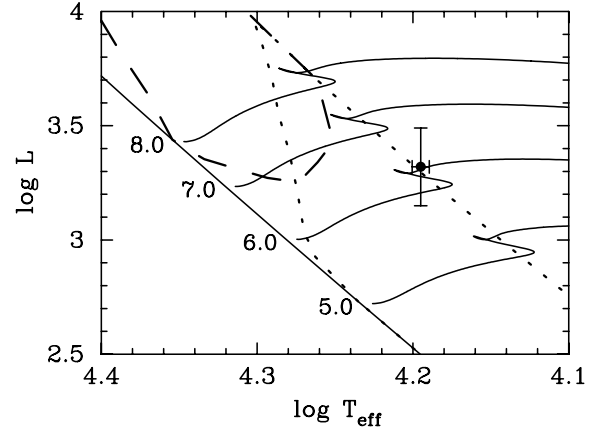


**Figure 5.** The position of  $\mu$  Eri in the theoretical HR diagram. Some stellar model evolutionary tracks labelled with their masses (full lines) for  $(v \sin i)_{\text{ZAMS}} = 200 \text{ km s}^{-1}$  are included. The theoretical borders of the  $\beta$  Cephei and SPB star instability strips (Pamyatnykh 1999; thick dashed and dotted lines, respectively) are included for comparison. The evolutionary tracks are shifted to the zero-age main sequence (ZAMS; full diagonal line) and to the instability strip boundaries because the latter do not include rotational effects.

excited which are so closely spaced in frequency that we cannot resolve them with the time base of our measurements.

However, pulsation is not the only possible physical cause of the light variations of  $\mu$  Eri. For the 1.622-d time-scale of the variability of the star to be due to rotational effects, an equatorial rotational velocity of  $193 \text{ km s}^{-1}$  is required. The published estimates of the projected rotational velocity  $v \sin i$  of  $\mu$  Eri range from  $150 \text{ km s}^{-1}$  (Abt et al. 2002) to  $190 \text{ km s}^{-1}$  (Bernacca & Perinotto 1970), which is consistent with that constraint. A double-wave light variation with twice that period would, however, be in conflict with the measured  $v \sin i$ . The complexity of the light variations of  $\mu$  Eri argues against a rotational origin.

The same argument can be used against an interpretation of  $\mu$  Eri’s variability in terms of binarity. In addition (as argued above for the long period detected for  $\nu$  Eri), the wavelength dependence of the colour amplitudes in our measurements suggests that a pure geometric origin of this variability is unlikely. Most importantly, however, the 7.3-d spectroscopic binary period of  $\mu$  Eri is quite different from the observed time-scale of its light variability or from an integral multiple of it.

Hence, we cannot unambiguously determine the cause of the variability of  $\mu$  Eri. A high-resolution, high S/N spectroscopic study will probably allow us to distinguish between the two viable hypotheses, pulsation or rotational modulation.

## 5 CONCLUSIONS

Our photometric multisite campaign of the  $\beta$  Cephei star  $\nu$  Eri has resulted in the largest single data set ever obtained for such a pulsator. The frequency analysis of these measurements has revealed the presence of eight independent pulsation modes, which is the most ever detected for such a star. These are normal  $\beta$  Cephei type variations (p and g modes of low radial order), but one additional signal may be a high-order gravity-mode pulsation.  $\nu$  Eri could therefore be not only a  $\beta$  Cephei star, but also an SPB star. It would thus be the second example of a star exhibiting two different types of pulsation. The high-order g-modes of the first such star, HD 209295, are however believed to be triggered by tidal effects (Handler et al.

2002). As we have no evidence for binarity of  $\nu$  Eri, it may therefore be the first star in which two types of pulsation with time-scales more than an order of magnitude different are intrinsically excited.

The  $\beta$  Cephei type pulsation frequencies show some regular structures, i.e. some are contained in multiplets that may be due to non-radial m-mode splitting. If so, the rotation period of  $\nu$  Eri is between 30–60 d, depending on the type of modes in these multiplets. These multiplets are a strong constraint for pulsational mode identification, which will be the subject of a future paper. In any case, the low-order p- and g-mode spectrum of  $\nu$  Eri as reported here is suitable for detailed seismic modelling.

## ACKNOWLEDGMENTS

This work has been supported by the Austrian Fonds zur Förderung der wissenschaftlichen Forschung under grant R12-N02. MJ's participation in the campaign was partly supported by KBN grant 5P03D01420. MJ would also like to acknowledge a generous allotment of telescope time and the hospitality of Lowell Observatory.

We thank the following students of the University of Hawaii for their assistance during some of the observations: Dan Bolton, Alexandre Bouquin, Josh Bryant, Thelma Burgos, Thomas Chun, Alexis Giannoulis, Marcus Lambert, Amanda Leonard, Alex MacIver, Danielle Palmese, Jennale Peacock, David Plant, Ben Pollard, Sunny Stewart, Dylan Terry and Brian Thomas.

GH wishes to express his thanks to Lou Boyd and Peter Reegen for their efforts in maintaining and controlling the Fairborn APTs, to Marcin Kubiak for supplying his archival measurements of  $\nu$  Eri, to Jan Cuypers for helpful information on the passbands of the archival data, and to Conny Aerts and Anamarija Stankov for comments on a draft version of this paper.

## REFERENCES

- Abt H. A., Levato H., Grosso M., 2002, *ApJ*, 573, 359  
Aerts C., Waelkens C., de Pauw M., 1994, *A&A*, 286, 136  
Aerts C., Thoul A., Daszyńska J., Scuflaire R., Waelkens C., Dupret M. A., Niemczura E., Noels A., 2003, *Sci*, 300, 1926  
Balona L. A., 2000, in Breger M., Montgomery M. H., eds, *ASP Conf. Ser. Vol. 210, Delta Scuti and Related Stars*. Astron. Soc. Pac., San Francisco, p. 170  
Bernacca P. L., Perinotto M., 1970, *Contr. Oss. Astrof. Padova in Asiago*, 239, 1B  
Breger M. et al., 1999, *A&A*, 349, 225  
Crawford D. L., 1978, *AJ*, 83, 48  
Cuypers J., Goossens M., 1981, *A&AS*, 45, 487  
Cuypers J., Aerts C., Buzasi D., Catanzarite J., Conrow T., Laher R., 2002, *A&A*, 392, 599  
Daszyńska-Daszkiewicz J., Dziembowski W. A., Pamyatnykh A. A., Goupil M.-J., 2002, *A&A*, 392, 151  
De Cat P., Aerts C., 2002, *A&A*, 393, 365  
de Jager C., 1963, *Bull. Astr. Inst., Netherlands*, 17, 1  
Drilling J. S., Landolt A. U., 2000, in Cox A. N., ed., *Allen's Astrophysical Quantities*, 4th edn. Springer Verlag, Berlin, p. 392  
Dziembowski W. A., Jerzykiewicz M., 2003, in Balona L. A., Henrichs H. F., Medupe R., eds, *ASP Conf. Ser. Vol. 305, Magnetic Fields in O, B and A Stars: Origin and Connection to Pulsation, Rotation and Mass Loss*. Astron. Soc. Pac., San Francisco, in press  
Dziembowski W. A., Pamyatnykh A. A., 1991, *A&A*, 248, L11  
ESA, 1997, *The Hipparcos and Tycho catalogues*, ESA SP-1200  
Flower P. J., 1996, *ApJ*, 469, 355  
Garrido R., Rodríguez E., 1996, *MNRAS*, 281, 696  
Handler G., 2003, *Baltic Astron.*, 12, 253  
Handler G., Aerts C., 2002, *Comm. Asteroseismology*, 142, 20  
Handler G. et al., 1996, *A&A*, 307, 529  
Handler G. et al., 1997, *MNRAS*, 286, 303  
Handler G. et al., 2000, *MNRAS*, 318, 511  
Handler G. et al., 2002, *MNRAS*, 333, 262  
Handler G., Shobbrook R. R., Vuthela F. F., Balona L. A., Rodler F., Tshenye T., 2003, *MNRAS*, 341, 1005  
Heynderickx D., Waelkens C., Smeyers P., 1994, *A&AS*, 105, 447  
Hill G., 1969, *Publ. DAO Victoria*, 13, 323  
Jerzykiewicz M., 1978, *Acta Astron.*, 28, 465  
Jerzykiewicz M., 1993, *Acta Astron.*, 43, 13  
Koen C., Eyer L., 2002, *MNRAS*, 331, 45  
Kubiak M., 1980, *Acta Astron.*, 30, 41  
Kubiak M., Seggewiss W., 1991, *Acta Astron.*, 41, 127  
Künzli M., North P., Kurucz R. L., Nicolet B., 1997, *A&AS*, 122, 51  
Lyngå G., 1959, *Arkiv Astron.*, 2, 379  
Martínez P., Koen C., 1994, *MNRAS*, 267, 1039  
Montgomery M. H., O'Donoghue D., 1999, *Delta Scuti Star Newsletter*, 13, 28  
Moskalik P., Dziembowski W. A., 1992, *A&A*, 256, L5  
Nather R. E., Winget D. E., Clemens J. C., Hansen C. J., Hine B. P., 1990, *ApJ*, 361, 309  
Pamyatnykh A. A., 1999, *Acta Astron.*, 49, 119  
Pamyatnykh A. A., 2002, *Comm. Asteroseismology*, 142, 10  
Pamyatnykh A. A., 2003, *Ap&SS*, 284, 97  
Sperl M., 1998, *MSc thesis*, Univ. Vienna  
Stankov A., Handler G., Hempel M., Mittermayer P., 2002, *MNRAS*, 336, 189  
Sterken C. et al., 1986, *A&AS*, 66, 11  
Wu Y., 2001, *MNRAS*, 323, 248  
van Hoof A., 1961, *Z. Astrophys.*, 53, 106  
Zima W. et al., 2002, in Aerts C., Bedding T. R., Christensen-Dalsgaard J., eds, *ASP Conf. Proc., Vol. 259, Radial and Nonradial Pulsations as Probes of Stellar Physics*. Astron. Soc. Pac., San Francisco, p. 598

This paper has been typeset from a  $\text{\TeX}/\text{\LaTeX}$  file prepared by the author.